The synthesis, crystal structure and vibrational spectra of α-$Sr(PO_3)_2$ containing an unusual *catena*-polyphosphate helix

Henning A. Höppe *

Institut für Anorganische und Analytische Chemie, Albert-Ludwigs-Universität, Albertstraße 21, D-79104 Freiburg, Germany

1. Introduction

Although phosphates are amongst the most thoroughly investigated compounds there is still a lack of knowledge about the structure of many crystalline phosphates. Among these, alkaline earth phosphates, for example, attract interest in materials science, e.g., due to the possibility of doping them with divalent or trivalent rare earth ions to produce efficient fluorescent materials [1]. Already in 1847 Maddrell reported some first details about the synthesis of strontium phosphate $Sr(PO_3)_2$ [2]. More than a century later, the powder diffraction patterns of three strontium *catena*-polyphosphates, namely α-, β- and γ-$Sr(PO_3)_2$, were described during the determination of the phase diagram of $SrO–P_2O_5$ [3]. It took almost another forty years until the first reports about their structures arose when Jansen et al. [4] and Olbertz et al. [5] disclosed the crystal structure of β-$Sr(PO_3)_2$ which is isotypic with that of $Pb(PO_3)_2$ [6]. Two years later, also the structure of γ-$Sr(PO_3)_2$ could be determined [7] and, moreover, a redetermination of β-$Sr(PO_3)_2$ was presented therein. Both are monoclinic with a monoclinic angle β close to 90°. This angle amounts to 90.62° [5] and 91.56° [7] for β-$Sr(PO_3)_2$ and γ-$Sr(PO_3)_2$, respectively. However, the deviations from 90° are apparently large enough to avoid major twinning problems. Up to now the crystal structure of the α-polymorph was still unknown and not even a unit cell had been proposed. In this contribution the solution of the crystal structure of pseudo-merohedrally twinned α-$Sr(PO_3)_2$ will be presented and compared with the two other polymorphs. Additionally, the vibrational spectra are reported.

2. Experimental

2.1. Synthesis

The synthesis of α-$Sr(PO_3)_2$ was performed in a tube furnace according to Eq. (1).

$$3SrCO_3 + 10H_3PO_3 \rightarrow 3\alpha\text{-}Sr(PO_3)_2 + 15H_2O + 4P + 3CO_2. \quad (1)$$

* Fax: +49-(0)761-203-6012.
E-mail address: henning.hoeppe@ac.uni-freiburg.de (H.A. Höppe).

Under argon a mixture of 89 mg (0.60 mmol) strontium carbonate (Alfa Aesar, 97.5%) and 164 mg (2.00 mmol) phosphorous acid (Riedel–de Haën, 98%) was transferred into an alumina boat. The latter was then heated under a nitrogen flow to 1150 K with a rate of 180 K h^{-1} and maintained at this temperature for 14 h until no further condensation of red phosphorus occurred. Then the mixture was cooled to room temperature with a rate of 180 K h^{-1} and yielded 146 mg single-phase α-$Sr(PO_3)_2$ as a crystalline, colourless and non-hygroscopic powder (0.595 mmol, yield: 99%).

2.2. *Vibrational spectroscopy*

An FTIR spectrum was obtained at room temperature by using a Bruker IFS 66v/S spectrometer. The samples were thoroughly mixed with dried KBr (approx. 2 mg sample, 300 mg KBr). Raman spectra were recorded by a Bruker FRA 106/S module with a Nd-YAG laser ($\lambda = 1064$ nm) scanning a range from 400 to 4000 cm^{-1}.

3. Crystal structure and crystallographic classification

3.1. *Crystal structure determination*

X-ray diffraction data of α-$Sr(PO_3)_2$ were collected on a Stoe IPDS-II diffractometer using Mo-K_α radiation. A suitable single crystal was enclosed in a Lindemann tube. The diffraction data were corrected for absorption by applying a numerical correction based on the measured crystal shape by the program X-Red (Stoe & Cie., Darmstadt, Germany).

Initial indexing of the single crystal data revealed a body-centred tetragonal unit cell ($a = 7.35$ Å, $c = 9.34$ Å). Oriented layers of the reciprocal space were calculated using IP data of a long-term single crystal X-ray measurement and revealed superstructure reflections (Fig. 1) which led to a doubling of c to give a primitive tetragonal unit cell ($a_{tetragonal} = 7.35$ Å, $c_{tetragonal} = 18.68$ Å). After a careful investigation the other axes remained unchanged. During the structure refinement of initial structure models two independent individuals were observed suggesting a twinning problem. To deal with this twinning the symmetry had to be reduced from tetragonal to monoclinic leading to the correct space group $P2_1$ (no. 4). To obtain the usual setting of space group $P2_1$, the axes $b_{tetragonal}$ and $c_{tetragonal}$ of the original tetragonal cell were swapped ($b = c_{tetragonal}$ and vice versa). The unit cell refinement was repeated and gave a monoclinic unit cell with an angle $\beta = 90.021(9)°$, very close to 90°. The applied twin law was a twofold rotational axis along b with an additional inversion twinning. Therefore, four individual pseudo-tetragonal merohedral twin domains of index 1 ($\sum = 1$, $\omega = 0$ [8]) had to be considered (i.e., called "Vierling"). During the refinement utilising the twinning matrix no merging of the reflections was allowed.

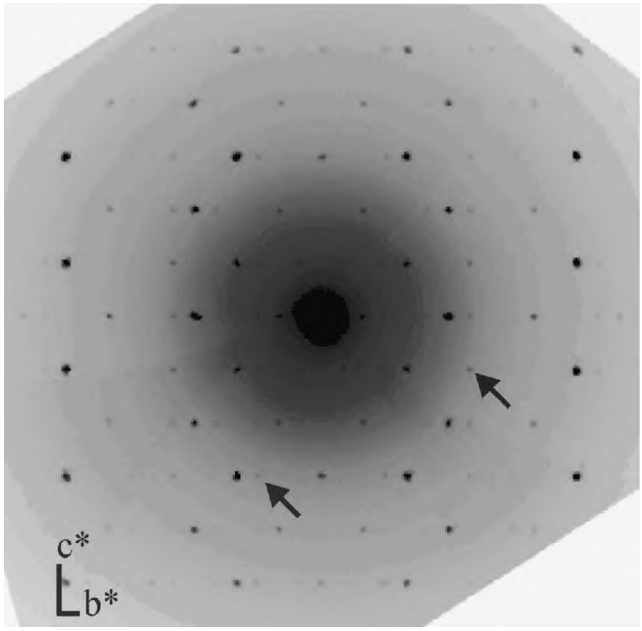

Fig. 1. Representation of the reciprocal lattice layer ($1kl$) calculated from IPDS data, typical superstructure reflections are indicated by arrows; the axes b^* and c^* are indicated according to the usual setting of $P2_1$.

The crystal structure of α-$Sr(PO_3)_2$ was solved by direct methods using SHELXTL [9] and refined with anisotropic displacement parameters for the strontium atoms. The relevant crystallographic data and further details of the X-ray data collection are summarised in Table 1. Table 2 shows the positional and displacement parameters for all atoms. In Table 3 selected interatomic distances and angles are listed. Due to the centred substructure cell and the weakness of the superstructure reflections a rather low signal-to-noise ratio was obtained. The additional twinning led to a stable but not as accurate as desirable refinement with comparably large standard deviations. Therefore, soft restraints were applied to the P–O bond lengths (P–O^{term} vs. P–O^{br}, br = bridging, term = terminal) and on the angles O^{term}–P–O^{term} to stabilise the structure refinement. Additionally, pairs of isotropic displacement parameters of chemically very similar phosphorus atoms (P1 and P5, P2 and P6, P3 and P7, P4 and P8) were refined together.

To confirm the obtained structure model a Rietveld refinement was performed. A sample of α-$Sr(PO_3)_2$ was enclosed in a glass capillary with 0.3 mm diameter and investigated at room temperature in Debye–Scherrer geometry on a STOE Stadi P powder diffractometer with Ge(111)-monochromatized Mo-K_α radiation (linear PSD detector, step width 0.5°, acquisition time: 2600 s/step). The powder diffraction pattern shows only minor amorphous contributions. All reflections have been indexed and their observed intensities are in very good agreement with the calculated diffraction pattern based on the single crystal data as well as the powder diffraction pattern recorded in 1959 [3]. The Rietveld refinement of the structure model (Fig. 2, Table 1) has been performed with the program GSAS [10,11] and

Table 1
Crystallographic data of α-$Sr(PO_3)_2$ (estimated standard deviations in parentheses)

Crystal data	
$Sr_4(PO_3)_8$	$F(000) = 928$
$M = 1964.48$ g/mol	$\rho_{X\text{-ray}} = 3.227$ g cm^{-3}
monoclinic	Mo-K_α-radiation
space group $P2_1$ (no. 4)	$\lambda = 0.71073$ Å
$a = 7.3537(8)$ Å	$\mu = 11.25$ mm^{-1}
$b = 18.682(2)$ Å $\quad \beta = 90.021(9)°$	$T = 293(2)$ K
$c = 7.3581(8)$ Å	crystal shape: rod
$V = 1010.9(2)$ Å^3	$0.02 \times 0.03 \times 0.08$ mm^3
$Z = 2$	colourless
Data collection	
Stoe IPDS-II	
absorption correction: numerical	$h = -8 \rightarrow 8$
$T_{min} = 0.5457$; $T_{max} = 0.7899$	$k = -22 \rightarrow 22$
$R_\sigma = 0.0768$	$l = -8 \rightarrow 8$
$2\theta_{max} = 50.0°$	7430 independent reflections per twin individual
	3263 observed reflections ($F_o^2 \geqslant 2\sigma(F_o^2)$)
Refinement	
refinement on F^2	program used to refine structure: SHELXL-97 [9]
$R1 = 0.0610$	$w^{-1} = \sigma^2 F_o^2 + (xP)^2 + yP$; $P = (F_o^2 + 2F_c^2)/3$
$wR2 = 0.1465$	weighting scheme (x/y) 0.0657/0
GooF = 0.978	twin fractions: 0.23(1), 0.22(1), 0.27(1), 0.28(1)
	twin type: pseudo-merohedral of index 1 ($\sum = 1$, $\omega = 0$ [8])
29 719 measured reflections	min. residual electron density: -1.11 e Å^{-3}
164 parameters	max. residual electron density: 2.31 e Å^{-3}
Powder diffraction (*Rietveld refinement*)	
STOE Stadi P, Debye–Scherrer geometry	program used: GSAS [10,11]
Mo-K_α-radiation, linear PSD detector	step width 0.5° / acquisition time: 2600 s/step
$a = 736.21(8)$ pm	$wR_P = 0.024$
$b = 1868.88(7)$ pm $\quad \beta = 90.130(6)°$	$R_P = 0.016$
$c = 735.65(5)$ pm	$R_{F^2} = 0.089$
	$R_F = 0.063$
refined parameters: structure 152; profile 18	$\chi^2 = 2.250$
	3767 reflections ($2\theta_{max} = 65.0°$)

confirms the single crystal data. The atomic parameters remain almost unchanged and therefore the detailed structural parameters are not reproduced herein.

3.2. The crystal structure

In the novel structure type of α-$Sr(PO_3)_2$ helical PO_3^- *catena*-polyphosphate ions interpenetrate a substructure of Sr^{2+} closely related to cubic diamond with Sr3 and Sr4 forming a tetragonally distorted face centred closest packing ($a_{Sr} \approx b_{Sr} = 10.40$ Å, $c_{Sr} = 9.34$ Å). Sr1 and Sr2 occupy half of all tetrahedral holes while the PO_3^- anion wriggles through the Sr substructure filling the octahedral and remaining tetrahedral voids (Fig. 3). O4 and O8 are situated in the remaining tetrahedral holes, O6 and O2 are located in the four octahedral holes.

The *catena*-polyphosphate chains consist of condensated PO_4 tetrahedra and form helices running along [010]. Their chain-periodicity $\boldsymbol{P}$ is 16 and the length of the repeating unit complies with $b = 1868$ pm (Fig. 4). The chain stretching factor [12] amounts to $f_s = 0.48$ assuming an average $l_T = 244.4$ pm, i.e., the length of a tetrahedron edge O^{br}–O^{br}, and $I_{chain} = 1868$ pm ($\boldsymbol{P} = 16$). This value is near the lower end of the range found in other chain polyphosphates ($f_s = 0.45 \ldots 1.0$, see below) and can be attributed to the high helical torsion of the polyphosphate chain.

Polyatomic chains can be described using an *IUPAC* nomenclature recommendation normally applicable for biopolymers [13]. Therein each bond between adjacent atoms B and C is denoted according to its torsion angle, i.e., the dihedral angle Θ ($0 \ldots \pm 180°$), of a chain of four atoms A–*B*–*C*–D. In the case of a chain of condensated PO_4 tetrahedra the chain is represented by the central P atoms only (Fig. 4). Subsequently, the torsion angles of the contact lines between neighbouring P atoms are calculated and classified using the symbols T (antiperiplanar, $\Theta \approx 180°$), C (synperiplanar, $\Theta \approx 0°$), G^+ or G^- (synclinal, $\Theta \approx \pm 60°$) and A^+ or A^- (anticlinal, $\Theta \approx \pm 120°$). Additionally, the local environments of the P atoms are described as cisoid (c, $\angle(PPP) \approx 90°$) or transoid (t, $\angle(PPP) \approx 180°$). If either positive or negative Θ prevail in a chain, chiral chains are formed. In α-$Sr(PO_3)_2$ all P centres are connected cisoid

Table 2
Atomic coordinates, their respective isotropic and anisotropic displacement parameters / Å^2 for α-$Sr(PO_3)_2$ (estimated standard deviations in parentheses); all atoms are on Wyckoff position 2*a*; c. n. = coordination number

atom[c. n.]	*x*	*y*	*z*	U_{11}	U_{22}	U_{33}	U_{23}	U_{13}	U_{12}	U_{eq}/U_{iso}
Sr1[8]	0.0059(3)	−0.7305(2)	−0.0024(3)	0.0255(13)	0.0243(14)	0.0162(10)	−0.0011(6)	−0.0043(10)	−0.0037(8)	0.0220(6)
Sr2[8]	0.5038(3)	−0.48255(13)	−0.5038(2)	0.0125(10)	0.0094(9)	0.0160(10)	0.0000(6)	−0.0102(9)	−0.0017(8)	0.0126(4)
Sr3[8]	0.0049(3)	−0.35659(10)	−0.4958(2)	0.0103(10)	0.0092(8)	0.0147(8)	0.0000(5)	−0.0061(9)	−0.0025(7)	0.0114(4)
Sr4[8]	0.5052(3)	−0.60664(10)	−0.0049(2)	0.0099(10)	0.0090(8)	0.0126(8)	0.0001(6)	−0.0053(9)	−0.0032(7)	0.0105(4)
P1[4]	−0.0009(6)	−0.5595(2)	0.0282(6)							0.0222(7)
O11^{term}	−0.1482(10)	−0.6048(6)	−0.0369(14)							0.013(3)
O12^{term}	0.1779(9)	−0.5886(6)	0.043(2)							0.023(3)
O1^{br}	−0.0672(14)	−0.5464(9)	−0.7662(7)							0.034(2)
P2[4]	−0.0090(6)	−0.5295(2)	−0.5592(6)							0.0085(5)
O21^{term}	−0.1632(10)	−0.4895(7)	−0.470(2)							0.026(3)
O22^{term}	0.1652(9)	−0.4895(6)	−0.550(2)							0.024(3)
O2^{br}	0.029(2)	−0.1062(3)	−0.526(2)							0.028(3)
P3[4]	−0.0503(8)	−0.1834(3)	−0.4998(7)							0.0151(8)
O31^{term}	−0.047(3)	−0.2202(7)	−0.6701(9)							0.031(4)
O32^{term}	0.035(2)	−0.2168(7)	−0.3422(12)							0.030(4)
O3^{br}	0.2487(9)	−0.6653(10)	−0.5799(12)							0.031(2)
P4[4]	0.4513(8)	−0.6542(2)	−0.5035(7)							0.0136(8)
O41^{term}	0.464(2)	−0.6047(6)	−0.3454(9)							0.020(3)
O42^{term}	0.542(2)	−0.6238(7)	−0.6700(10)							0.026(3)
O4^{br}	0.469(3)	−0.2310(3)	−0.528(2)							0.051(6)
P5[4]	0.4865(6)	−0.3088(3)	−0.4501(7)							0.0222(7)
O51^{term}	0.3471(12)	−0.3482(7)	−0.545(2)							0.027(4)
O52^{term}	0.6689(9)	−0.3372(7)	−0.444(2)							0.029(4)
O5^{br}	0.4080(12)	−0.2913(6)	−0.2530(6)							0.019(2)
P6[4]	0.5134(5)	−0.7790(2)	−0.9461(5)							0.0085(5)
O61^{term}	0.3465(9)	−0.7336(6)	−0.960(2)							0.015(3)
O62^{term}	0.6713(9)	−0.7486(6)	−0.0476(14)							0.015(3)
O6^{br}	0.466(2)	−0.8556(3)	−0.022(2)							0.021(3)
P7[4]	0.4530(7)	−0.4340(3)	−0.9864(5)							0.0151(8)
O71^{term}	0.541(2)	−0.4780(6)	−0.8506(10)							0.014(3)
O72^{term}	0.441(2)	−0.4601(6)	−0.1708(8)							0.020(3)
O7^{br}	−0.2517(8)	−0.9192(8)	−0.0842(15)							0.034(2)
P8[4]	−0.0505(7)	−0.9043(2)	−0.0138(5)							0.0136(8)
O81^{term}	−0.048(2)	−0.8629(7)	0.1597(8)							0.020(3)
O82^{term}	0.0438(15)	−0.8651(5)	−0.1653(8)							0.010(2)
O8^{br}	−0.028(2)	−0.4804(2)	−0.037(2)							0.029(3)

to their respective phosphor neighbours, and along the chain T- and A-type contact lines alternate (the relevant angles are listed in Table 4). Furthermore, three positive Θ outbalance one negative Θ giving an unusual chiral helix:

$$|{:}c_{(P1)} - T - c_{(P2)} - A^+ - c_{(P3)} - T - c_{(P4)} - A^+$$
$$-c_{(P5)} - T - c_{(P6)} - A^- - c_{(P7)} - T - c_{(P8)} - A^+{:}|.$$

Recently, Snir and Kamien determined the optimum pitch to radius ratio for helix formation based on a simulation with small hard spheres and rod-like molecules to be $\xi^* = 2.5122$ [14]. In the PO_3^- helix this ratio amounts to $\xi = 18.68/7.499 = 2.49$ in excellent accordance with ξ^*. This result seems interesting since the simulation was done with the aim to describe the screwing of large biomolecules within cells.

The bond lengths P–O^{term} ranging from 142.7(5) to 151.0(5) pm (average 147 pm) are significantly shorter than the bond lengths P–O^{br} (156.8(4)–160.9(4) pm, average 159 pm). They agree well with typical bond lengths inside

Table 3
Selected interatomic distances/pm and angles/° for α-$Sr(PO_3)_2$ (estimated standard deviations in parentheses)

Sr1–O^{term}	243.6(8)–295.7(12)	8 distances
Sr2–O^{term}	246.5(8)–300.7(14)	8 distances
Sr3–O^{term}	249.5(6)–287.7(13)	8 distances
Sr4–O^{term}	245.6(7)–303.4(12)	8 distances
Sr–Sr	434.0(3)–438.0(3)	
P–O^{term}	142.7(5)–151.0(5)	∅ = 147.0
P–O^{br}	156.8(4)–160.9(4)	∅ = 158.5
O^{term}–P–O^{br}	99.9(6)–121.6(9)	∅ = 109.5
O^{term}–P–O^{term}	111.9(5)–119.4(5)	∅ = 115.7
O^{br}–P–O^{br}	96.1(8)–106.3(9)	∅ = 101.3
P–O^{br}–P	136.8(7)–146.9(7)	∅ = 139.7

Table 4
Torsion angles/° in the helix in α-$Sr(PO_3)_2$ of the respective bond

P1	P2	P3	P4	P5	P6	P7	P8	P1
	−163.8		−164.8		−175.9		+172.3	
		90.3		92.3		−91.9		92.6

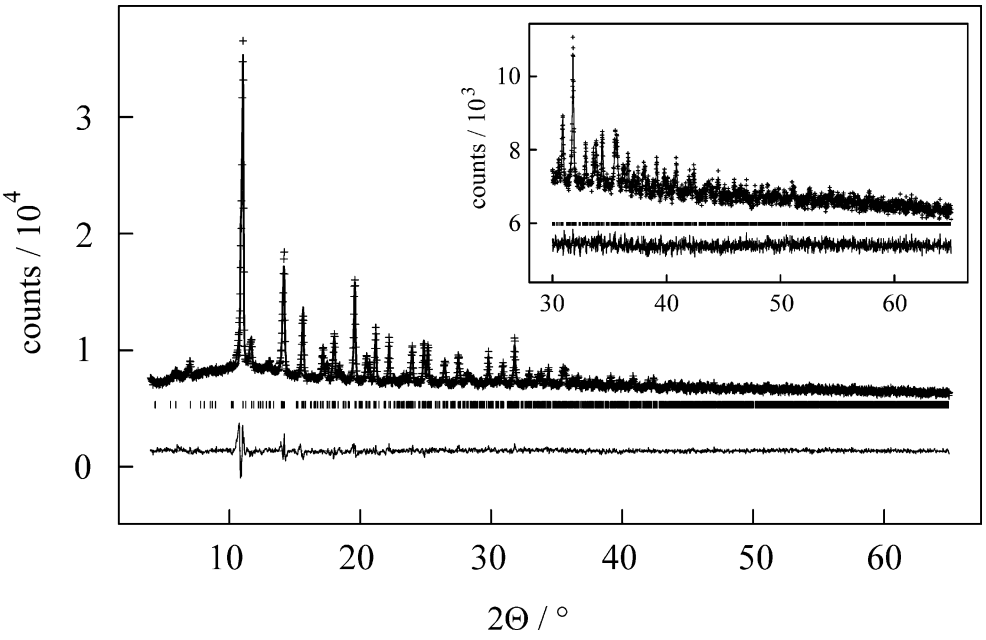

Fig. 2. Observed (crosses) and calculated (line) X-ray powder diffraction pattern (Mo-K_α radiation) as well as the difference profile of the Rietveld refinement of α-$Sr(PO_3)_2$. The row of vertical lines indicate possible peak positions of α-$Sr(PO_3)_2$.

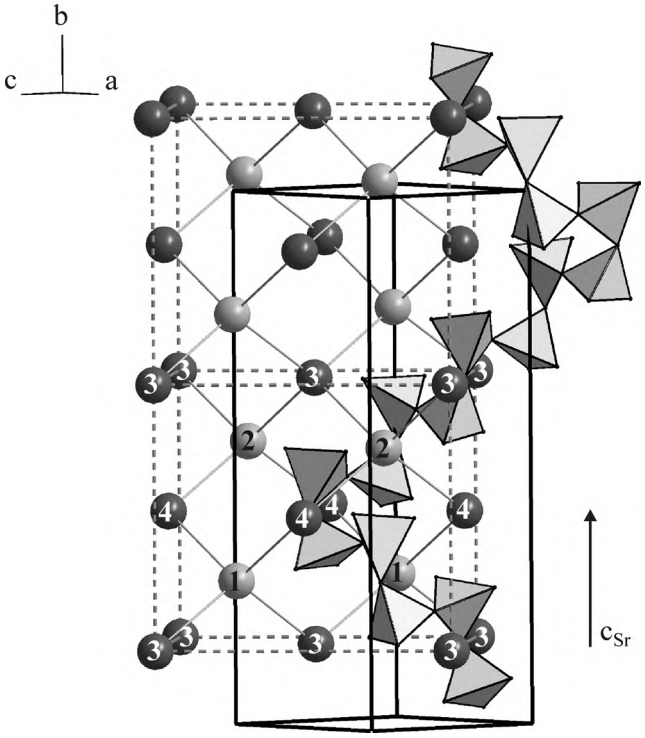

Fig. 3. Virtual cell (dotted, a_{SR}, b_{SR}, c_{SR}) of the diamond like substructure of Sr^{2+} interpenetrated by a PO_3^- helix (the "bonds" connecting Sr^{2+} ions visualise the diamond like network and do not represent bonds in a chemical sense, the PO_4 tetrahedra are shown as closed polyhedra); the numbers indicate the respective Sr site.

phosphate chains in other *catena*-phosphates [4–7,15,16]. As observed previously in these *catena*-phosphates, the angles O^{br}–P–O^{br} are significantly smaller compared with the angles O^{term}–P–O^{term} presumably due to a partial double–bond character of the P–O^{term} bonds. This observation holds also for α-$Sr(PO_3)_2$.

All four crystallographically independent Sr^{2+} ions are coordinated by terminal oxygen atoms O^{term} only, the distances Sr–O vary between 243.6(8) and 303.4(12) pm with an average value of 267 pm in good agreement with the sum of ionic radii of 261 pm [17]. The Sr^{2+} are eightfold coordinated and exhibit a very similar coordination geometry. Four of the eight oxygen atoms deviate only slightly from a tetragonal plane through the central Sr^{2+}, above and below of which the other four oxygen atoms are positioned in a strongly compressed tetrahedral arrangement (Fig. 5).

Further details of the crystal structure investigations may be obtained from the Fachinformationszentrum Karlsruhe, Abt. PROKA, D-76344 Eggenstein-Leopoldshafen, Germany (e-mail: crysdata@fiz-karlsruhe.de) on quoting the depository number CSD-415334, the name of the author, and citation of this publication.

3.3. *Comparison with β-$Sr(PO_3)_2$ and γ-$Sr(PO_3)_2$*

The most evident difference between α-$Sr(PO_3)_2$ and the other polymorphic forms β-$Sr(PO_3)_2$ and γ-$Sr(PO_3)_2$ is probably the different coiling of the PO_3^- polyphosphate chains decreasing from α-$Sr(PO_3)_2$ ($\boldsymbol{P} = 16$, Fig. 4) via β-$Sr(PO_3)_2$ ($\boldsymbol{P} = 4$) to the almost stretched anion in the γ-polymorph with $\boldsymbol{P} = 2$ (Fig. 6). Accordingly, f_s increases in the same direction (α-$Sr(PO_3)_2$: 0.48, β-$Sr(PO_3)_2$: 0.85, γ-$Sr(PO_3)_2$: 0.93). The chain stretching factors of homologue polyphosphates are 0.70 and 0.93 in the case of $Ba(PO_3)_2$ [18,19] and 0.71 for $Ca(PO_3)_2$ [20], respectively. In the high-temperature polymorph of $Be(PO_3)_2$ III a rather low f_s of 0.45 due to a strong folding of the polyphosphate

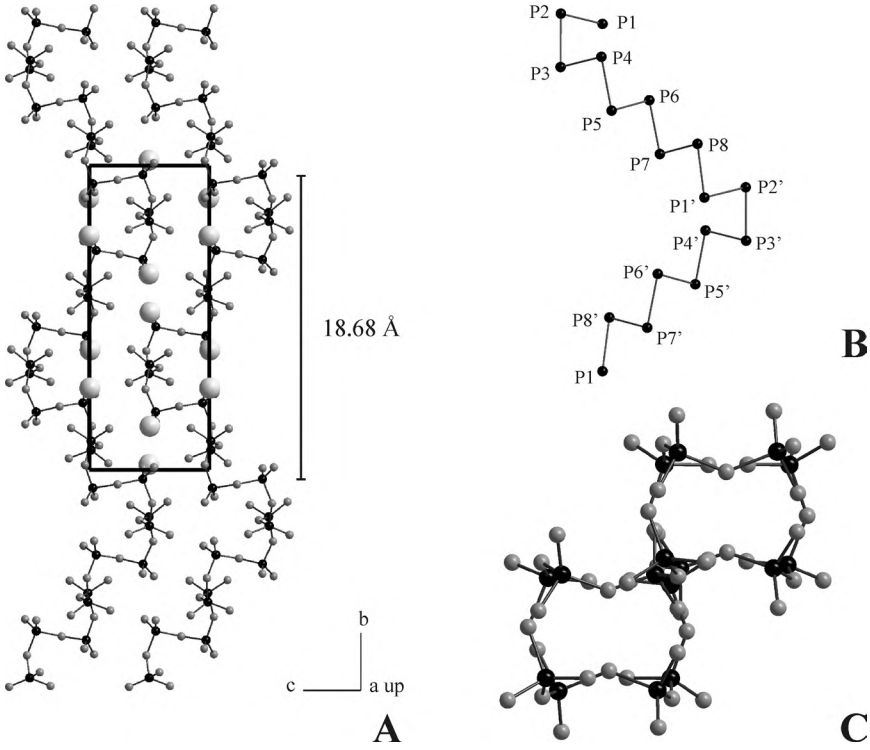

Fig. 4. The helical anion PO_3^- in α-$Sr(PO_3)_2$ (P: black, O: dark grey, Sr: grey); A: view along [100], B: view along [101] shows only the P atoms (the "bonds" connecting P visualise the topology between the polyhedra and do not represent bonds in a chemical sense), C: view of a single chain along [010].

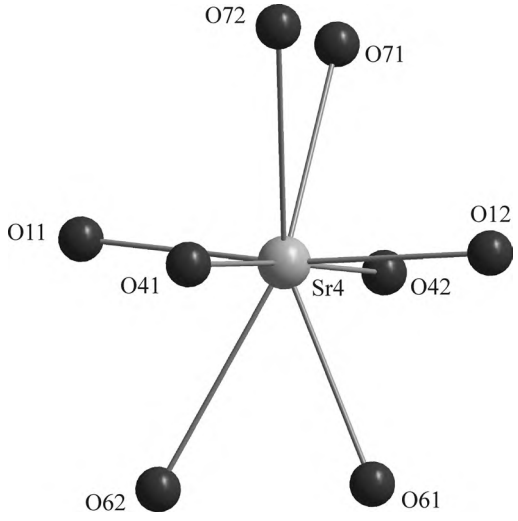

Fig. 5. Representation of the coordination environment of Sr4 in α–$Sr(PO_3)_2$ (Sr: grey, O: dark grey).

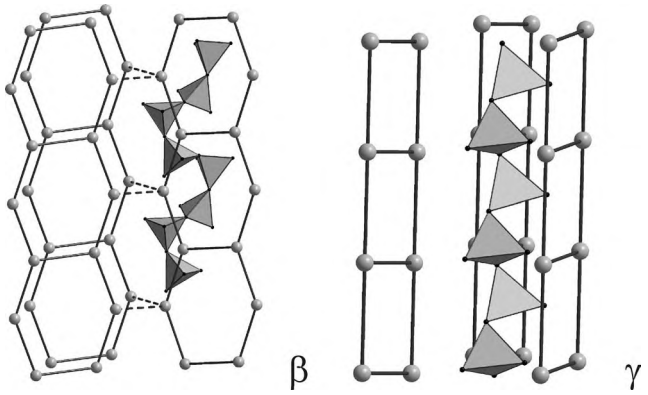

Fig. 6. Comparison of the *catena*-polyphosphate chains embedded in their respective Sr^{2+} substructure in β- and γ-$Sr(PO_3)_2$ (from left).

chain has been found [21]. In this case, though, the Be^{2+} are tetrahedrally coordinated. Completely stretched chains of condensated PN_4 tetrahedra were described in Ca_2PN_3 [22,23].

The coordination numbers (c. n.) as well as the mean coordination distances of Sr^{2+} are very similar in α-$Sr(PO_3)_2$ (c. n. 8, $\varnothing_{Sr-O} = 267$ pm), β-$Sr(PO_3)_2$ (c. ns. 8 and 7 + 1, $\varnothing_{Sr-O} = 263$ pm) and the γ-polymorph (c. n. 8, $\varnothing_{Sr-O} = 265$ pm). The Sr^{2+} substructures however show significant differences. In γ-$Sr(PO_3)_2$ the Sr^{2+} form chains of square planar annellated four-rings ($d_{Sr-Sr} \approx 420$ pm) with large distances beyond 5 Å to adjacent ones while in β-$Sr(PO_3)_2$ chains of almost planar annellated six-rings ($d_{Sr-Sr} \approx 380 \ldots 400$ pm) of Sr^{2+} find neighbouring chains already within a distance of about 480 pm forming corrugated six-rings (Fig. 6). Hence the latter shows already a slight relationship to the diamond-like Sr^{2+} substructure in α-$Sr(PO_3)_2$ where the distances of adjacent Sr^{2+} differ within the small range from 434.0(3) to 438.0(3) pm.

Therefore the main structure influencing motif in the sequence γ-, β- and α-polymorph seems to be the Sr^{2+} substructure which strives for an increasing symmetry with

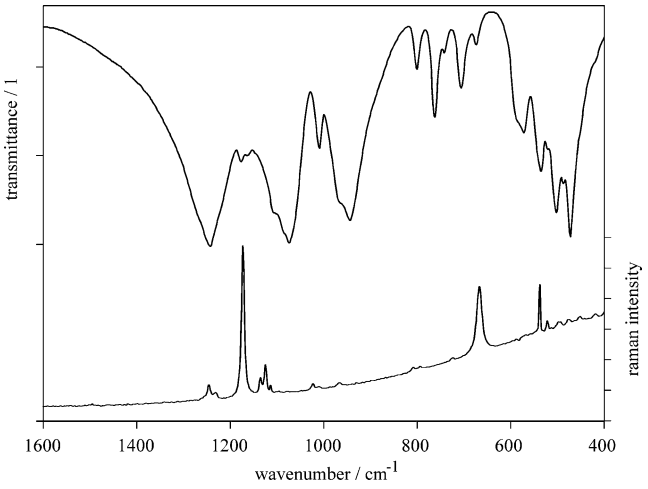

Fig. 7. Infrared and Raman vibrational spectra of α-$Sr(PO_3)_2$.

smallest distance differences as possible. Consequently, the polyphosphate chain is increasingly coiled.

4. Vibrational spectroscopy

Fig. 7 shows the IR and Raman spectra of the title compound α-$Sr(PO_3)_2$. The IR spectra of *catena*-polyphosphates are not significantly different from those of *catena*-oligophosphates [24]. The only characteristic bands should be found in the region between 800 and 650 cm^{-1}, where the number of bands should correspond to the periodicity of the phosphate chain. Unfortunately, this holds quite reliably only for low chain periodicities. In α-$Sr(PO_3)_2$, the characteristic frequencies of *catena*–polyphosphate chains such as the $\nu_{as}(PO_2)$ are detected between 1200 and 1310 cm^{-1} with a maximum at 1243 cm^{-1}, the very intense ν_{as}(POP) at 944 cm^{-1} and $\nu(PO^{term})$ ranging from 1019 up to 1100 cm^{-1}. Additionally, the Raman spectra of α-$Sr(PO_3)_2$ show strong vibrations in the region around 1173 ($\nu_s(PO^{term})$), and at 667 cm^{-1} (ν_s(POP)). Thus the observed vibrational data are in good agreement with the expected values.

Acknowledgements

The author thanks Mrs. A. Becherer, Albert-Ludwigs-Universität Freiburg, for recording the vibrational spectra and Prof. Dr. H. Hillebrecht, Institut für Anorganische und Analytische Chemie, Albert-Ludwigs-Universität Freiburg, for valuable discussions and generous support.

References

[1] G. Blasse, J. Alloys Compd. 192 (1993) 17.
[2] R. Maddrell, Lieb. Ann. Chem. 61 (1847) 53.
[3] R.C. Ropp, M.A. Aia, C.W.W. Hoffman, T.J. Veleker, R.W. Mooney, Anal. Chem. 31 (1959) 1163.
[4] M. Jansen, N. Kindler, Z. Kristallogr. 212 (1997) 141.
[5] A. Olbertz, D. Stachel, I. Svoboda, H. Fuess, Z. Kristallogr. 212 (1997) 135.
[6] K.H. Jost, Acta Crystallogr. 17 (1964) 1539.
[7] M. Graia, A. Driss, T. Jouini, Acta Crystallogr. C 55 (1999) 1395.
[8] R.W. Cahn, Adv. Phys. 3 (1954) 363.
[9] G.M. Sheldrick, SHELXTL, v.5.10 Crystallographic System, Bruker AXS Analytical X-Ray Instruments Inc., Madison, 1997.
[10] R.B. von Dreele, A.C. Larson, General Structure Analysis System (GSAS), Los Alamos National Laboratory Report LAUR 86-748, 2000.
[11] B.H. Toby, J. Appl. Crystallogr. 34 (2001) 210.
[12] F. Liebau, Structural Chemistry of Silicates, Springer-Verlag, Berlin, 1985.
[13] A.D. McNaught, A. Wilkinson, IUPAC Compendium of Chemical Terminology, Blackwell Science, Oxford, 1997.
[14] Y. Snir, R.D. Kamien, Science 307 (2005) 1067.
[15] H.A. Höppe, Z. Anorg. Allg. Chem. 631 (2005) 1272.
[16] W.H. Baur, Acta Crystallogr. B 30 (1974) 1195.
[17] R.D. Shannon, C.T. Prewitt, Acta Crystallogr. B 25 (1969) 925.
[18] P.J. Coing-Boyat, M.T. Averbuch-Pouchot, J.C. Guitel, Acta Crystallogr. B 34 (1978) 2689.
[19] J.C. Grenier, C. Martin, A. Durif, T.Q. Duc, J.C. Guitel, Bull. Soc. Franc. Mineral. Cristallogr. 90 (1967) 24.
[20] M. Schneider, K.H. Jost, P. Leibnitz, Z. Anorg. Allg. Chem. 527 (1985) 99.
[21] E. Schultz, F. Liebau, Z. Kristallogr. 154 (1981) 115.
[22] W. Schnick, V. Schultz-Coulon, Angew. Chem. Int. Ed. Engl. 32 (1993) 280.
[23] V. Schultz-Coulon, W. Schnick, Z. Anorg. Allg. Chem. 623 (1997) 69.
[24] A. Rulmont, R. Cahay, M. Liegeois-Duyckaerts, P. Tarte, Eur. J. Solid State Inorg. Chem. 28 (1991) 207.